

This is the peer reviewed version of the following article: Controlling the Electrical Properties of Undoped and Ta-doped TiO₂ Polycrystalline Films via Ultra-Fast Annealing Treatments, by Piero Mazzolini, Tolga Acartürk, Daniel Chrastina, Ulrich Starke, Carlo Spartaco Casari, Giuliano Gregori, Andrea Li Bassi, Advanced Electronic Materials 2016, 1500316, which has been published in final form at DOI: 10.1002/aelm.201500316 . This article may be used for non-commercial purposes in accordance with [Wiley Terms and Conditions for Self-Archiving](#).

Advanced Electronic Materials

Controlling the Electrical Properties of Undoped and Ta-doped TiO₂ Polycrystalline Films via Ultra-Fast Annealing Treatments --Manuscript Draft--

Manuscript Number:	aelm.201500316R1
Full Title:	Controlling the Electrical Properties of Undoped and Ta-doped TiO ₂ Polycrystalline Films via Ultra-Fast Annealing Treatments
Article Type:	Full Paper
Section/Category:	
Keywords:	Transparent conducting oxides; pulsed laser deposition; anatase; defect chemistry; perovskite-based solar cells.
Corresponding Author:	Andrea Li Bassi Politecnico di Milano Milano, ITALY
Corresponding Author Secondary Information:	
Corresponding Author's Institution:	Politecnico di Milano
Corresponding Author's Secondary Institution:	
First Author:	Piero Mazzolini
First Author Secondary Information:	
Order of Authors:	Piero Mazzolini Tolga Acartürk Daniel Chrastina Ulrich Starke Carlo Spartaco Casari Giuliano Gregori Andrea Li Bassi
Order of Authors Secondary Information:	
Abstract:	<p>We present a study on the crystallization process of undoped and Ta doped TiO₂ amorphous thin films. In particular, the effect of ultra-fast annealing treatments in environments characterized by different oxygen concentrations is investigated via in-situ resistance measurements. The accurate examination of the key parameters involved in this process allows us to reduce the time needed to obtain highly conducting and transparent polycrystalline thin films (resistivity $\sim 6 \times 10^{-4} \Omega\text{cm}$, mean transmittance in the visible range $\sim 81\%$) to just 5 minutes (with respect to the 180 minutes required for a "standard" vacuum annealing treatment) in nitrogen atmosphere (20 ppm oxygen concentration) at ambient pressure. Experimental evidence of superficial oxygen incorporation in the thin films and its detrimental role for the conductivity are obtained by employing different concentrations of traceable ¹⁸O isotopes during ultra-fast annealing treatments. The results are discussed in view of the possible implementation of the ultra-fast annealing process for TiO₂-based transparent conducting oxides as well as electron selective layers in solar cell devices; taking advantage of the high control of the ultra-fast crystallization processes which has been achieved, these two functional layers are shown to be obtainable from the crystallization of a single homogeneous thin film.</p>
Additional Information:	
Question	Response

Please submit a plain text version of your cover letter here.

Please note, if you are submitting a revision of your manuscript, there is an opportunity for you to provide your responses to the reviewers later; please do not add them to the cover letter.

Dear Editor,

we submit our manuscript 'Controlling the Electrical Properties of Undoped and doped TiO₂ Polycrystalline Films via Ultra-Fast Annealing Treatments' by P. Mazzolini, T. Acartürk, D. Chrastina, U. Starke, C.S. Casari, G. Gregori and A. Li Bassi to be considered for publication in *Advanced Functional Materials*. The paper presents several novel aspects regarding the tunability of the electrical properties of TiO₂ thin films that are certainly of great interest for the broad community dealing with this material.

The first novelty concerns the ability of studying the crystallization process of amorphous undoped and Ta-doped TiO₂ thin films, while monitoring in situ their electrical resistance during ultra-fast annealing treatments. This was possible thanks to the fabrication of a dedicated halogen-lamps-based furnace, which allowed extremely rapid heating and cooling ramps in controlled atmospheres.

The second and extremely relevant aspect of this work is the achievement of highly conducting ($\rho \sim 6 \times 10^{-4} \Omega\text{cm}$) and transparent (transmittance in the visible region exceeding 80%) thin films by employing a very short (just 5 minutes) temperature cycle (up to 460 °C) in a low purity nitrogen atmosphere at ambient pressure. In order to grasp the technological importance of such a result, one should note that the conventional annealing treatments on amorphous TiO₂-based thin films (which are routinely performed in vacuum or hydrogen atmosphere) require an overall thermal cycle of several hours (up to $T \sim 550$ °C) in order to obtain the same functional properties of our films. We thus demonstrate the possibility to decouple the TiO₂ functional properties from the annealing environment.

Finally, the systematic investigation of in situ electrical data during ultra-fast annealing treatments performed in different nitrogen-oxygen mixtures gave us the possibility of identifying the key role played by the incorporation of oxygen (and thus the crucial role of the oxygen partial pressure) and, in particular, in which way this could affect the electrical properties of TiO₂-based thin films. Aimed experiments (e.g. secondary ion mass spectroscopy in depth profiles on Ta-doped TiO₂ films, which were crystallized in ultra-fast treatments in the presence of traceable ¹⁸O) enabled to correlate the superficial oxygen incorporation to the decreased amount of conduction electrons in the superficial layer of titania films.

In summary, apart from the evident technological relevance of such a fast treatment performed in low purity nitrogen at atmospheric pressure (which in principle could be industrially scalable for several TiO₂ applications), we are confident that this work represents an important further step towards a better understanding of the interplay between material properties and its interaction with the environment. Furthermore, we believe that the high control level which has been achieved for this ultra-fast process can disclose also interesting and novel perspectives for application in innovative solar cell devices (e.g. perovskite-based solar cells).

Sincerely yours,
Andrea Li Bassi

DOI: 10.1002/ ((please add manuscript number))

Article type: **Full Paper**

Controlling the Electrical Properties of Undoped and Ta-doped TiO₂ Polycrystalline Films via Ultra-Fast Annealing Treatments

Piero Mazzolini, Tolga Acartürk, Daniel Chrastina, Ulrich Starke, Carlo Spartaco Casari, Giuliano Gregori[†] and Andrea Li Bassi*[†]*

P. Mazzolini

1) Department of Energy - Politecnico di Milano, via Ponzio 34/3, I-20133 Milano, Italy. 2) Center for Nano Science and Technology - IIT@PoliMI, Via Pascoli 70/3, I-20133 Milano, Italy.

T. Acartürk

3) Max Planck Institute for Solid State Research, Heisenbergstr. 1, 70569 Stuttgart, Germany.

Dr. D. Chrastina

4) L-NESS, Dipartimento di Fisica, Politecnico di Milano - Polo Territoriale di Como, Via Anzani 42, I-22100 Como, Italy

Prof. Dr. U. Starke

3) Max Planck Institute for Solid State Research, Heisenbergstr. 1, 70569 Stuttgart, Germany.

Prof. Dr. C. S. Casari

1) Department of Energy - Politecnico di Milano, via Ponzio 34/3, I-20133 Milano, Italy. 2) Center for Nano Science and Technology - IIT@PoliMI, Via Pascoli 70/3, I-20133 Milano, Italy.

Dr. G. Gregori

3) Max Planck Institute for Solid State Research, Heisenbergstr. 1, 70569 Stuttgart, Germany.

E-mail: g.gregori@fkf.mpg.de

tel.: +497116891770

Prof. Dr. A. Li Bassi

1) Department of Energy - Politecnico di Milano, via Ponzio 34/3, I-20133 Milano, Italy. 2) Center for Nano Science and Technology - IIT@PoliMI, Via Pascoli 70/3, I-20133 Milano, Italy.

E-mail: andrea.libassi@polimi.it

tel.: +390223996316

[†] The two authors contributed equally to the manuscript

Keywords: transparent conducting oxides, pulsed laser deposition, anatase, defect chemistry, perovskite-based solar cells

We present a study on the crystallization process of undoped and Ta doped TiO₂ amorphous thin films. In particular, the effect of ultra-fast annealing treatments in environments

1 characterized by different oxygen concentrations is investigated via *in-situ* resistance
2 measurements. The accurate examination of the key parameters involved in this process
3
4 allows us to reduce the time needed to obtain highly conducting and transparent
5
6 polycrystalline thin films (resistivity $\sim 6 \times 10^{-4} \Omega\text{cm}$, mean transmittance in the visible range
7
8 $\sim 81\%$) to just 5 minutes (with respect to the 180 minutes required for a “standard” vacuum
9
10 annealing treatment) in nitrogen atmosphere (20 ppm oxygen concentration) at ambient
11
12 pressure. Experimental evidence of superficial oxygen incorporation in the thin films and its
13
14 detrimental role for the conductivity are obtained by employing different concentrations of
15
16 traceable ^{18}O isotopes during ultra-fast annealing treatments. The results are discussed in view
17
18 of the possible implementation of the ultra-fast annealing process for TiO_2 -based transparent
19
20 conducting oxides as well as electron selective layers in solar cell devices; taking advantage
21
22 of the high control of the ultra-fast crystallization processes which has been achieved, these
23
24 two functional layers are shown to be obtainable from the crystallization of a single
25
26 homogeneous thin film.
27
28
29
30
31
32
33
34

35 **1. Introduction**

36 TiO_2 is one of the key materials for energy applications such as lithium-ion batteries,
37
38 photocatalysis, water splitting, and charge carrier separation/collection in solar cells.^[1] If we
39
40 consider photovoltaic applications, TiO_2 in the anatase phase is the most employed material
41
42 for several architectures of dye sensitized and perovskite-based solar cells:^[2-4] this is mainly
43
44 related to a high chemical stability, its intrinsic transparency to visible light (bandgap $E_g = 3.2$
45
46 $- 3.4 \text{ eV}$ ^[5, 6]) and to the favorable energy level alignment at the solar cell interfaces, which
47
48 enables an efficient and selective charge carrier uptake and transport (n-type charge transport
49
50 as a photoanode and/or as a hole-blocking, electron selective layer) from the photoactive
51
52 material to the front transparent electrode of the solar cell.^[7, 8] This electrode is generally a
53
54 thin film of a transparent conducting oxide (TCO), usually fluorine-doped tin oxide (FTO).^[9]
55
56
57
58
59
60
61
62
63
64
65

1
2
3
4
5
6
7
8
9
10
11
12
13
14
15
16
17
18
19
20
21
22
23
24
25
26
27
28
29
30
31
32
33
34
35
36
37
38
39
40
41
42
43
44
45
46
47
48
49
50
51
52
53
54
55
56
57
58
59
60
61
62
63
64
65

However, the discovery of donor doped TiO₂ as a promising new class of n-type TCO,^[10] and the possibility of obtaining highly conducting and transparent polycrystalline Nb or Ta-doped TiO₂ (TaTO) thin films on inexpensive glass substrates, open up new opportunities for a better suited energy level alignment at the device interfaces via an all TiO₂-based configuration (photoanode/selective layer and TCO).^[11-13] Between the two mentioned donor doped compositions, Ta-doped TiO₂ is thought to have several advantages with respect to the more widely investigated Nb for transparent conductor applications, namely higher mobility and dopant solubility.^[14] Moreover, it has been suggested that donor-doped TiO₂ could be a superior material compared to undoped TiO₂ not only as a TCO but also as an electron selective layer (i.e. hole blocking layer) and photoanode.^[15-17] In both cases the chosen material must provide efficient electron transport pathways, combined with a low charge carrier density, in order to reduce the recombination rate with the photogenerated charges.^[18] It is important to mention that depending on the adopted synthesis conditions (reducing vs. oxidizing deposition/annealing atmosphere) it is possible to finely tune the mobile charge carrier density in TiO₂-based films as well as their functional (electrical/optical) properties.^[12, 15] Typically, in order to achieve the highest electrical conduction upon deposition, TiO₂-based thin films require an annealing process in a reducing atmosphere (vacuum or H₂-based atmosphere, commonly at temperatures between 500 °C and 600 °C) so as to induce crystallization to a pure anatase phase and thus increase the carrier mobility, without compromising the charge carrier density.^[12, 13, 19] In this context, it is noteworthy that annealing processes in oxidizing atmospheres (e.g. air) result in highly insulating films.^[12] Although such a result is expected from defect chemistry considerations, the exact mechanisms underlying this process and involving different phenomena (crystallization, oxygen incorporation) are still debated especially in the case of donor-doped TiO₂.^[20-27] In this contribution, we focus on how the post-deposition annealing treatments performed in different atmospheres and different heating/cooling rates affect the electrical properties of

undoped as well as tantalum doped anatase TiO₂ thin films. More importantly, we investigate the role of the change of the microstructure (from amorphous to crystalline) and of the oxygen exchange with the surroundings on the final electrical conductivity of the material. For this purpose, we consider amorphous films grown via pulsed laser deposition (PLD) at room temperature on soda lime glass substrates. We show that ultra-fast-annealing treatments (UFA: heating rate of 300 K/min up to the peak temperature of 460 °C and total treatment time of ~ 5 minutes) performed in a N₂ atmosphere (with 20 ppm O₂ concentration) at ambient pressure allow high quality transparent and conducting anatase thin films to be obtained. In particular, UFA-treated tantalum doped (TaTO) films show practically identical electrical and optical properties ($\rho_{\min} \sim 6 \times 10^{-4} \Omega\text{cm}$, transmittance in the visible range $T_{\text{vis}} \sim 81\%$) as TaTO layers, which were treated according to a vacuum annealing cycle which was already shown to be effective for obtaining the best optical and conduction properties (in this work this will be referred to as “standard annealing cycle”: $p < 4 \times 10^{-5}$ Pa, overall time heating + dwell at 550 °C + cooling ~ 180 minutes^[12]). It is worth mentioning that a previous study on Nb-doped TiO₂ thin films reported on the possibility of obtaining good resistivity values ($\rho = 8.4 \times 10^{-4} \Omega\text{cm}$) upon annealing in a diluted atmosphere (0.5 atm) of highly pure nitrogen (purity 99.9998%, nominal oxygen concentration < 0.5 ppm) at 350 °C for 20 minutes.^[28] The physicochemical mechanisms behind this result (e.g. role of possible oxygen incorporation during annealing) were however not discussed.

Here instead in-situ electrical measurements carried out during UFA enable us to study the thin film crystallization process, and to identify the threshold limit of oxygen concentration for which the electrical properties start to be negatively affected for Ta-doped and undoped TiO₂. In order to investigate the possible oxygen incorporation/diffusion into the films during annealing, we perform time-of-flight secondary ion mass spectrometry (TOF-SIMS) on TaTO samples crystallized using UFA under different ¹⁸O concentrations (80 ppm and 1000 ppm). This also allows us to deconvolve the role of the crystallization process from the annealing

1 atmosphere on the final electrical properties of the films. Finally, the findings are discussed
2 also in view of the possible technological implications in the field of next generation solar
3
4 cells.
5
6
7

8 **2. Materials and Methods**

9

10 **2.1 Thin Film Deposition**

11 Amorphous Ta-doped TiO₂ (TaTO) and TiO₂ thin films were grown by room temperature
12 PLD on soda-lime glass (10 × 10 × 1 mm³) and Si (100) substrates at room temperature in the
13 presence of an oxygen background pressure of about 1 Pa (TaTO was deposited at 1 Pa, while
14 TiO₂ at 1.25 - 1.3 Pa). Ablation was performed from TiO₂ (powder purity 99.9%) or
15 Ta₂O₅:TiO₂ (molar ratio of 0.025:0.975, powder purity 99.99%) targets to deposit TiO₂ or
16 TaTO films, respectively. A ns-pulsed Nd:YAG laser (4th harmonic, $\lambda = 266$ nm) with a
17 repetition rate $f_p = 10$ Hz, a pulse duration of ~ 6 ns and a laser fluence of 1.15 J/cm² was
18 used. The target-to-substrate distance was fixed at 50 mm.
19
20
21
22
23
24
25
26
27
28
29
30
31
32
33
34
35

36 **2.2 Structural Characterization**

37 The film thickness was evaluated by means of scanning electron microscopy (Zeiss SUPRA
38 40 field-emission SEM) on samples grown on silicon. The crystalline structure was
39 determined by X-ray diffraction (PANalytical X'Pert PRO MRD high-resolution X-ray
40 diffractometer, using CuK _{α 1} radiation ($\lambda = 0.15406$ nm) selected by a two-bounce Ge
41 monochromator). XRD measurements were performed in both θ - 2θ and grazing incidence
42 angle configuration (fixed incidence angle $\omega = 5^\circ$). The thin film surfaces were investigated
43 by means of optical microscopy using polarized light (Leica DM2500 M). Optical
44 transmittance spectra (in the range 250 - 2000 nm) were evaluated with a UV-vis-NIR
45 PerkinElmer Lambda 1050 spectrophotometer with a 150 mm diameter integrating sphere. All
46 the acquired spectra were normalized with respect to the glass substrate contribution.
47
48
49
50
51
52
53
54
55
56
57
58
59
60
61
62
63
64
65

2.3 Thin Film Crystallization

1 As-deposited TiO₂ and TaTO thin films were annealed in a standard vacuum ($p < 4 \times 10^{-5}$ Pa,
2
3 obtained with an Agilent Varian Turbo-V 250 Turbomolecular Pump) or nitrogen (99.999 %
4
5 purity, oxygen concentration nominally < 3 ppm) atmosphere (1 atm, obtained after previous
6
7 vacuum at $p < 4 \times 10^{-5}$ Pa) in a home-made furnace at 550°C (10 K/min ramps) for 1 hour and
8
9 used as reference samples, according to reference^[12]. The resistivity, mobility and charge
10
11 carrier density were evaluated via Hall measurements (DC 4-point probe configuration) at
12
13 room temperature with a Keithley K2400 Source/Measure Unit as a current generator (from
14
15 100 nA to 10 mA), an Agilent 34970A voltage meter, and a 0.57 T Ecopia permanent magnet.
16
17
18 The crystallization process of the amorphous TiO₂-based thin films was studied with ultra-fast
19
20 annealing (UFA) consisting of ultra-fast temperature ramps (300 K/min) up to the peak
21
22 temperature of 460 °C (without dwell time) in a home-made furnace employing 5 IR lamps
23
24 (RS Components Ltd. UK, Heat lamp 500 W R7s 230 V) chosen to avoid any UV emission,
25
26 concentrically placed outside the chamber. The UFA treatments were performed at ambient
27
28 pressure under different oxygen/nitrogen mixtures (oxygen concentrations: 20 ppm, 1000 ppm
29
30 and 21%, which were monitored with a Cambridge Sensotec RapidOX 2100ZF lambda
31
32 sensor). The 20 ppm gas was obtained by directly employing nitrogen from the lab
33
34 distribution line, while the 1000 ppm and 21% mixtures were obtained by properly mixing N₂
35
36 and O₂ from a 5.0 purity oxygen bottle. The background gas was continuously flowing in the
37
38 chamber with a fixed flux of 50 sccm. The temperature was measured using a K-type
39
40 thermocouple (diameter 0.5 mm) placed on the sample holder at 0.5 mm from the substrate.
41
42
43 The furnace design allows also for a fast cooling ramp (about 150 K/min), which can be
44
45 achieved by an external flux of cold N₂ gas. The total treatment time (heating + cooling)
46
47 required for a typical UFA experiment was around 5 minutes. Changes of the thin film
48
49 electrical resistance were recorded *in-situ* through 2-point DC measurements (source/measure
50
51 unit Keithley 2604B). The maximum applied current was 1 mA and the maximum compliance
52
53
54
55
56
57
58
59
60
61
62
63
64
65

1 voltage 5 V. In order to minimize the effect of different contact geometries among different
2 samples, Ti/Au (200/2000 Å) electrodes with 1 mm distance from each other were evaporated
3
4 on top of the amorphous films. All the analyzed samples showed an ohmic behavior when
5
6 electrically measured between the two evaporated contacts. UFA treatments were also
7
8 performed on both TaTO and TiO₂ thin films without employing evaporated electrodes, in
9
10 order to subsequently measure their optical and electrical properties via *ex-situ* 4-point
11
12 configuration Hall measurements with contacts placed on the top surface. This allowed for a
13
14 direct comparison of these samples with those which are prepared according to the standard
15
16 annealing process.
17
18
19
20
21
22
23

24 **2.4 Tracing of Oxygen Incorporation**

25
26 In order to trace the oxygen incorporation we performed UFA on TaTO thin films in ¹⁸O
27
28 containing N₂ atmospheres (~80 ppm and ~1000 ppm, respectively). The ¹⁸O/¹⁶O
29
30 concentration profiles as a function of depth were obtained by Secondary Ion Mass
31
32 Spectrometry, using a commercial TOF-SIMS IV. The secondary ions were generated by
33
34 short pulses of a 25 keV Ga ion beam. Removal of material for depth profiling was carried out
35
36 using a second ion beam from a Cs source operated at 500 eV. The correlation between the
37
38 secondary ion extraction and depth was established using a Dektak 8 profilometer at the end
39
40 of the measurement.
41
42
43
44

45
46 The possible presence of an insulating top layer corresponding to superficial oxygen
47
48 penetration was investigated by removing the first tens of nm of an UFA-treated TaTO film
49
50 by bombardment by Ar ions at 0.2 kV accelerating voltage. The sputtering time was
51
52 calibrated by SEM images.
53
54
55
56
57

58 **3. Results**

1 Room temperature PLD of both TiO₂ and TaTO yields thin films characterized by absence of
2 long range crystalline order, as discussed in our previous work.^[12] The thickness of all the
3 analyzed films is 150 +/- 5 nm, as measured by SEM. The resistivity of all the as-deposited
4 thin films is about 10 Ωcm, with no particular dependence on the presence of doping; for as-
5 deposited films it was not possible to discern the contributions of charge carrier concentration
6 and charge mobility because of the highly scattered values obtained in Hall measurements.
7
8
9
10
11
12
13
14
15
16

17 3.1 Standard Annealing Process

18 A standard post deposition annealing process (i.e. $T = 550$ °C for 1 hour with heating and
19 cooling rates of 10 K/min) was performed on undoped and Ta-doped TiO₂ amorphous films in
20 vacuum, since this is a well-established procedure for obtaining highly conducting and
21 transparent polycrystalline anatase films.^[12] The room temperature resistivity of TaTO thin
22 films was one order of magnitude lower with respect to TiO₂ ($\rho = 6.77 \times 10^{-4}$ Ωcm and $6.93 \times$
23 10^{-3} Ωcm respectively). This is not surprising, as Ta substituting Ti in the anatase cell is an
24 electron donor, resulting in a larger concentration of mobile electrons ($n = 7.99 \times 10^{20}$ cm⁻³
25 and 5.70×10^{19} cm⁻³ for TaTO and TiO₂ respectively).^[20] On the other hand, the room
26 temperature mobility value is slightly higher for the undoped sample ($\mu = 11.5$ cm²V⁻¹s⁻¹ and
27 15.8 cm²V⁻¹s⁻¹ for TaTO and TiO₂ respectively). Nonetheless, one should note here that both
28 values belong to the best mobility range for TiO₂-based polycrystalline films.^[12] We observe
29 that, even though migration of atomic species from the glass substrate (e.g. Na) into the film
30 cannot be excluded a priori, no significant effects on the observed change of electrical
31 properties are expected; in fact the same annealing procedure on Ta-doped TiO₂ films
32 deposited on crystalline quartz led to negligible differences in the detected electrical
33 properties. The mean transmittance values in the visible range (T_{VIS} evaluated in the range 400
34 – 700 nm) are both within the important technological range for transparent electronics of
35 80% (81.4% and 79.3% for TaTO and TiO₂ respectively).^[29]
36
37
38
39
40
41
42
43
44
45
46
47
48
49
50
51
52
53
54
55
56
57
58
59
60
61
62
63
64
65

1 The TiO₂-based thin films were also annealed using a standard annealing process in 1 atm of
2 pure nitrogen gas (grade 99.999 %, nominal O₂ concentration < 3 ppm). The resulting
3
4 resistance of the thin films treated in N₂ was however too large for our experimental setup
5
6 (maximum applicable current of 0.1 μA, voltage compliance 10 V) and thus no value of the
7
8 resistivity could be determined.
9
10

11 **3.2 Ultra-Fast Annealing**

12 Since an abrupt drop in the electrical resistivity during the heat treatment of amorphous TiO₂-
13
14 based thin films was already proposed to be a sign of its crystallization,^[13, 27] the analysis of
15
16 the resistance behavior of the thin films recorded via *in-situ* electrical measurements during
17
18 the UFA treatments permits the threshold temperature and the time needed to crystallize the
19
20 amorphous thin films in the presence of different oxygen concentrations to be identified. The
21
22 acquired data for doped and undoped TiO₂ samples are plotted in **Figure 1** and **Figure 2**
23
24 (electrical resistance represented by dots linked to left y-axes, measured temperature
25
26
27
28
29
30
31
32
33
34
35
36
37
38
39
40
41
42
43
44
45
46
47
48
49
50
51
52
53
54
55
56
57
58
59
60
61
62
63
64
65

represented by dashed lines linked to right y-axes both as a function of time).

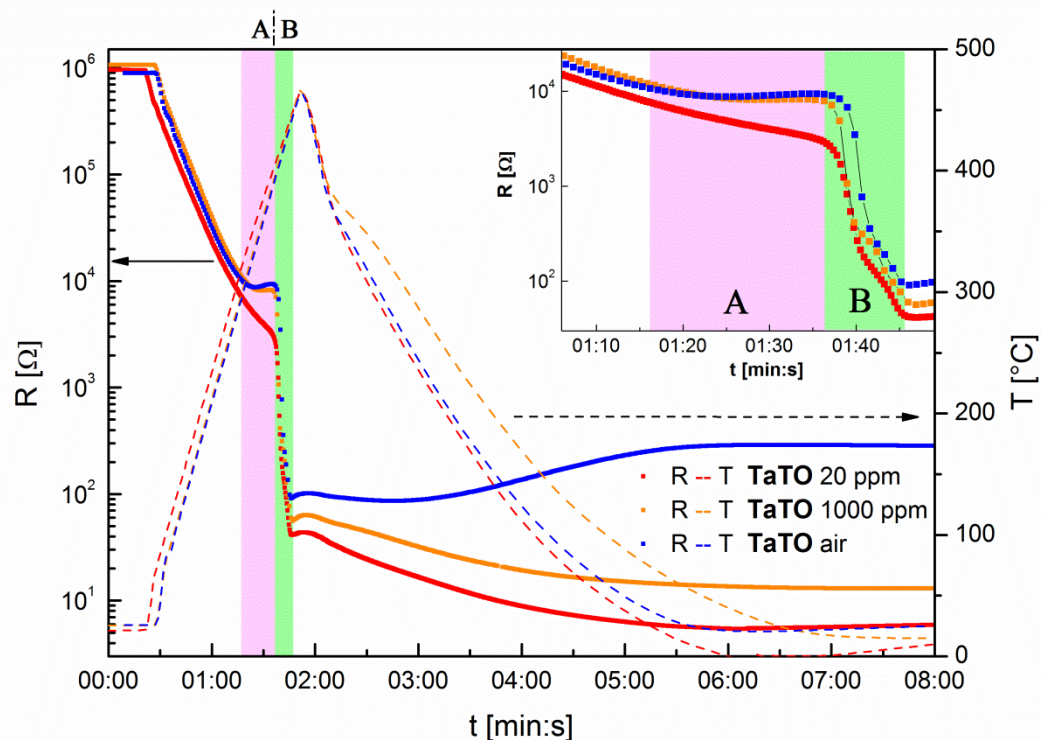


Figure 1. In-situ resistance measurements (dots, left y-axes) and corresponding temperature profiles (dashed lines, right y-axes) for TaTO thin films crystallized in N_2 -based atmospheres with different oxygen concentrations: 20 ppm (red), 1000 ppm (orange) and 21% (synthetic air, blue) atmospheres. The regions A and B (pink and green colored regions respectively) represent the time intervals in which the resistivity of the thin films starts to be affected by the presence of different p_{O_2} (A) and the time intervals in which the abrupt resistance drop takes place (B). In the inset is reported a magnification of the resistance behavior in the regions A and B.

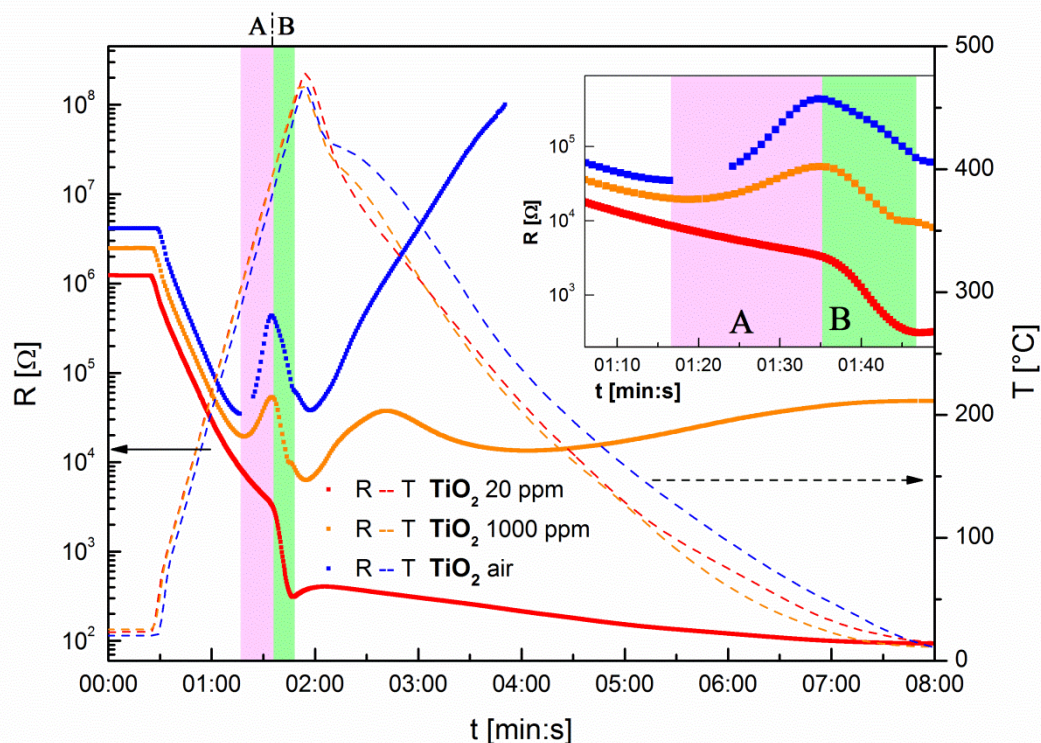


Figure 2. In-situ resistance measurements (dots, left y-axes) and corresponding temperature profiles (dashed lines, right y-axes) for TiO₂ thin films crystallized in N₂-based atmospheres with different oxygen concentrations: 20 ppm (red), 1000 ppm (orange) and 21% (synthetic air, blue) atmospheres. The regions A and B (pink and green colored regions respectively) represent the time intervals in which the resistivity of the thin films starts to be affected by the presence of different pO₂ (A) and the time intervals, in which the abrupt resistance drop takes place (B). In the inset is reported a magnification of the of the resistance behavior in the regions A and B. There are no resistance points for an electrical resistance higher than $1 \times 10^8 \Omega$ (blue dots) since this is the upper limit measurable with our experimental setup.

Irrespective of the presence of the dopant or the exposure to different annealing atmospheres, all the performed UFA treatments show an abrupt and sharp decrease of the resistance once a temperature of around 400 °C is reached. As was already mentioned, this transition is likely to be connected to the crystallization process of the amorphous films, the occurrence of which is highlighted in Figure 1 and 2 by the area in green (called region-B).^[13] Interestingly, the temperature and time values defining this green zone (T_{start} , T_{end} and t_{start} , t_{end}) appear to be very similar for TiO₂ and TaTO thin films: the T_{start} and T_{end} of this process are at around 400 °C and 450 °C respectively ($t_{start} - t_{end} = 10$ s) for all the investigated samples. It is possible to estimate the abrupt drop in the electrical resistance in region-B to be on the order

of a factor of 10 for TiO₂, and 100 for TaTO, although here the temperature dependence of the electrical resistance (dR/dT) is not taken into account ($\Delta T \sim 50$ °C).

Remarkably, the UFA performed in N₂ atmosphere (with 20 ppm O₂, red curves in Figure 1 and 2), resulted in low resistance TiO₂-based thin films showing a metallic behavior in the cooling region ($dR/dT > 0$). The obtained room temperature resistance ($R_{T=25^\circ C}$) for TaTO is one order of magnitude lower than for TiO₂ (6 Ω and 96 Ω, respectively). It is important to note that this difference is of the same order of magnitude of that obtained upon standard annealing treatments carried out in vacuum.

Nevertheless, a substantial difference in the resistance behavior during the heating cycle, also confirmed by the resistance values measured at room temperature, is observed when the UFA experiment is carried out in a more oxygen rich environment. In the case of TaTO, UFA performed in an N₂-based atmosphere with 1000 ppm O₂ (orange curves in Figure 1), resulted in a more than doubled $R_{T=25^\circ C}$ (13 Ω with respect to the 6 Ω obtained in 20 ppm of oxygen). Nevertheless the thin film maintained a metallic behavior during cooling as shown in Figure 1 for $t > 2$ min. In contrast, the crystallization process performed in the same conditions for TiO₂ resulted in a semiconducting behavior during cooling ($dR/dT < 0$, orange curves in Figure 2 for $t > 4$ min) while the $R_{T=25^\circ C}$ is orders of magnitude higher than for the UFA treatment carried out under 20 ppm of oxygen (4.2×10^4 Ω vs. 96 Ω). The effect of a further increase of the oxygen concentration is shown for UFA performed in an artificial air atmosphere (21% O₂ in N₂, blue curves in Figure 1 and 2). The electrical properties of both TaTO and TiO₂ thin films are significantly different compared to those of the films which were ultra-fast-annealed in 20 and 1000 ppm of oxygen. As a matter of fact, the resulting $R_{T=25^\circ C}$ was increased up to 278 Ω for TaTO, while for TiO₂ it was too high to be measurable with our experimental setup ($R > 10^8$ Ω).

We found that the increasing loss of conductivity with increasing O₂ concentration was associated with a different resistance behavior recorded before the abrupt resistance drop in

1 region-B. This is evident in the A-regions (highlighted in pink) in the UFA graphs shown in
2 Figure 1 and 2. In fact the resistance change with increasing temperature for the amorphous
3 samples treated under 20 ppm O₂ (red curves in Figure 1 and 2) could be defined as an
4 almost-monotonic decrease of resistance until the abrupt drop begins (region-B). In contrast,
5 for UFA performed under higher oxygen partial pressures (1000 ppm and air – 21%, orange
6 and blue curves respectively in Figure 1 and 2), a resistance increase in the region-A is
7 recorded. Moreover, it is interesting to note that the time interval (and consequently also the
8 ΔT) associated with this phenomenon is again similar for TaTO and TiO₂ thin films, although
9 this effect is definitely much more pronounced for the undoped samples ($t_{start} - t_{end} \sim 20$ s;
10 $T_{start} \sim 300$ °C, $T_{end} \sim 400$ °C).

11 Extended UFA treatments were performed in order to investigate the effect on the resistance
12 of a longer exposure (10 min) to 20 ppm O₂ at the peak temperature (460 °C). Note that all the
13 other parameters were kept constant (ambient pressure, 20 ppm O₂ in N₂, and the same
14 heating and cooling rates as in the conventional UFA treatments). The results, which are
15 shown in the Supporting Information (**Figure s1**), clearly indicate that a longer exposure to O₂
16 at 460 °C led to the degradation of the electrical conductivity of both TaTO and TiO₂ thin
17 films ($R_{T=25^\circ C} = 11 \Omega$ and 4965Ω for TaTO and TiO₂ respectively) with respect to the
18 conventional UFA cycle ($R_{T=25^\circ C} = 6 \Omega$ and 96Ω for TaTO and TiO₂ respectively).

19 We also performed the UFA treatments on samples without electrodes, in order to properly
20 compare their optical and electrical properties (4-point van der Pauw – Hall resistivity
21 measurements) with the samples prepared by the standard annealing process performed under
22 vacuum and N₂. Once annealed, the room temperature electrical properties obtained for TaTO
23 and TiO₂ thin films are stable in time (samples measured over several months), regardless of
24 the different temperature cycle employed (standard or UFA). UFA treatment of TaTO in 1
25 atm of hydrogen-containing atmosphere (Ar/H₂ mixture, H₂ at 2% - measured oxygen

concentration $< 10^{-20}$ ppm) was performed and compared to the standard vacuum annealing process.

Table 1. Electrical properties of TaTO and TiO₂ thin films evaluated via 4-point electrical measurements at room temperature. The “/” symbol means that it was not possible to obtain a reliable experimental value due to the highly scattered collected data. The “n. m.” abbreviation indicates that the samples were too insulating to be measurable with our experimental setup. The background colors used in the rows referring to N₂-based UFA treatments correspond to those in Figure 1 and 2.

	Annealing treatment	ρ [Ωcm]	n [cm^{-3}]	μ [$\text{cm}^2\text{V}^{-1}\text{s}^{-1}$]
TaTO	Standard-Vacuum	6.77×10^{-4}	7.99×10^{20}	11.5
	Standard-N ₂	n. m.	n. m.	n. m.
	UFA – Ar/H ₂	7.65×10^{-4}	7.46×10^{20}	11.0
	UFA – 20 ppm	6.85×10^{-4}	8.30×10^{20}	11.0
	UFA – 1000 ppm	/	/	/
	UFA - air	/	/	/
TiO ₂	Standard Vacuum	6.93×10^{-3}	5.70×10^{19}	15.8
	Standard N ₂	n. m.	n. m.	n. m.
	UFA – 20 ppm	9.04×10^{-3}	4.77×10^{19}	14.5
	UFA – 1000 ppm	n. m.	n. m.	n. m.

Notably, the ultra-fast-annealed TaTO film in reducing atmosphere (Ar/H₂) and the film crystallized in 20 ppm O₂ have electrical properties almost identical to those obtained with a standard vacuum annealing (see **Table 1**). In the case of TiO₂, the UFA treatment performed in 20 ppm of oxygen resulted in a slightly higher resistivity, although the overall electrical properties are comparable. On the other hand, a standard annealing process performed in a highly pure N₂ atmosphere (O₂ < 3 ppm) results in an insulating film (ρ not measurable). Moreover, it is worth mentioning that in the case of UFA treatments performed with O₂ concentrations of 1000 ppm and 21% on TaTO samples without electrodes, a notable increase

of the resistivity with respect to the best recorded values was recorded ($3.39 \times 10^{-3} \Omega\text{cm}$ and $2.31 \times 10^{-2} \Omega\text{cm}$ for 1000 ppm and 21% respectively). Nonetheless, these data have to be considered as only indicative due to the diode-like IV characteristics between the electrical probes and the sample, which invalidates the 4-point measurement method, and are consequently not reported in Table 1. On the other hand, in the case of TiO_2 , a UFA treatment in presence of 1000 ppm of oxygen was sufficient to result in an insulating film (ρ not measurable).

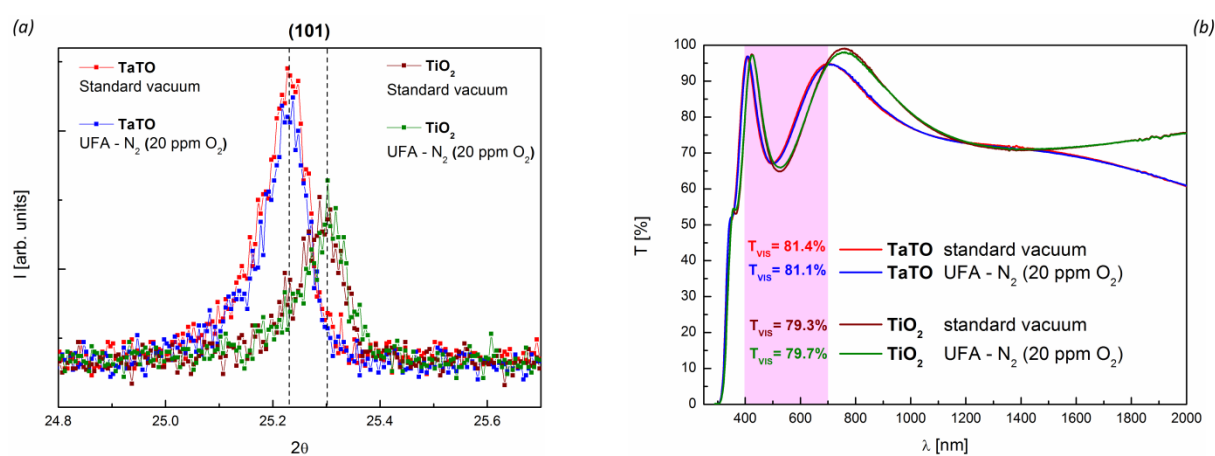


Figure 3. (a) the XRD acquisition for the (101) anatase peak in grazing incident angle ($\omega = 5^\circ$) is reported for 150 nm thick TaTO and TiO_2 films annealed with a standard vacuum (red and purple colored lines for TaTO and TiO_2 respectively) and an ultra-fast annealing (UFA) treatment in N_2 with 20 ppm of oxygen (blue and green colored lines for TaTO and TiO_2 respectively). (b) the total transmittance spectra for the same samples are reported (colors in agreement with (a)); the pink shaded part of the graph shows the visible region (400-700 nm) and the mean transmittance in the visible region (T_{vis}) is reported.

There is no significant difference in the crystallinity quality of TaTO and TiO_2 samples when annealed with the standard annealing or the UFA treatment, as indicated by the comparison between the most intense (101) XRD anatase signal (**Figure 3 (a)**). The variation in both the intensity ratio and the absolute 2θ positions of anatase X-ray peaks between TaTO and TiO_2 is consistent with a doping effect or with a defect-induced lattice distortion (or disordering), as discussed in reference^[12]. A complete θ - 2θ scan (reported in the Supporting Information, **Figure s2**) does not show the presence of other TiO_2 polymorphs (e.g. rutile), or any other segregated phase (e.g. metallic Ta or Ta_2O_5). Moreover, the presence of N_2 in the annealing

1 atmosphere (in both UFA and standard cycles) does not significantly hinder the crystallization
2 of the thin films, since the anatase phase was formed in all cases.

3
4 Consistently with the XRD data, also the optical properties of doped and undoped anatase
5 samples are shown to be independent of the employed thermal cycle. Quite remarkably,
6
7 despite the significantly lower temperature and shorter time, the UFA treatment is not
8
9 detrimental to the optical transparency of the crystallized thin films as shown by the
10
11 superimposed transmittance curves for TaTO and TiO₂ after standard vacuum annealing
12
13
14
15
16
17 **(Figure 3 (b))**. In particular, the mean optical transmittance in the visible range of TiO₂ and
18
19 TaTO reaches and exceeds the TCO technological limit of 80%.^[29]

22 23 **3.3 Oxygen Incorporation From the Crystallization Environment**

24
25 In order to further study the effect of oxygen on the final electrical properties, we performed
26
27 UFA treatments under nitrogen containing different ¹⁸O concentrations. This allowed us to
28
29 trace the oxygen penetration into TaTO thin films via depth profiles of the ¹⁸O/¹⁶O isotope
30
31 ratio obtained with TOF-SIMS.

32
33
34
35 The *in-situ* electrical measurements recorded during UFA treatments performed in nitrogen
36
37 atmosphere with 80 ppm and 1000 ppm of ¹⁸O are reported in **Figure 4 (a)** (purple and orange
38
39 curves respectively). Note that the mixture of N₂ with 80 ppm of ¹⁸O was used as it was the
40
41 lowest ¹⁸O concentration obtainable with our experimental setup. Let us consider region-A of
42
43 Figure 4 (a) first: here it is possible to observe that the increase from 20 to 80 ppm of oxygen
44
45 is already enough to affect the resistance behavior of the TaTO thin film. In line with the data
46
47 discussed above (Figure 1), the further increase up to 1000 ppm of ¹⁸O leads to an increased
48
49 resistance, although the metallic behavior of the thin film is preserved. The resulting $R_{T=25^{\circ}C}$
50
51 are 7 Ω and 10 Ω for 80 ppm and 1000 ppm ¹⁸O respectively.

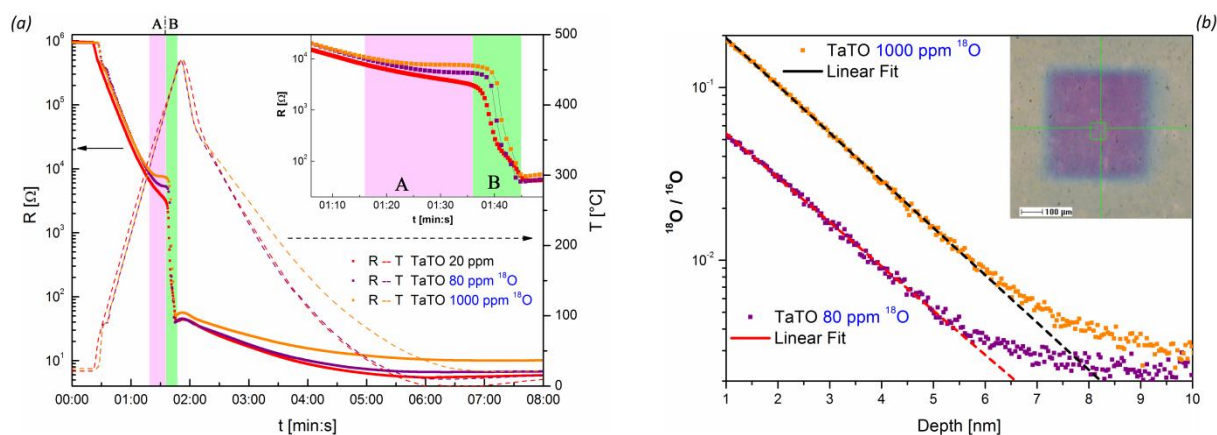


Figure 4. (a) In-situ resistance measurements (dots, left y-axes) and corresponding temperature cycles (dashed lines, right y-axes) for TaTO thin films crystallized in N_2 -based atmospheres with different ^{18}O concentrations: 80 ppm (purple) and 1000 ppm (orange). TaTO thin film crystallized in N_2 -based atmosphere with 20 ppm of oxygen (red) is reported as reference (already reported in Figure 1). The regions A and B (pink and green colored regions respectively) represent the time intervals in which the resistivity of the thin films starts to be affected by the presence of different oxygen concentrations (A) and in which the abrupt resistance drop takes place (B). In the inset a magnification of the resistance behavior in the regions A and B is reported. (b) the depth profile of the $^{18}O/^{16}O$ ratio traced via TOF-SIMS is reported; the colors of the dotted profiles are consistent with those used in (a); in the inset is reported an optical microscope acquisition of the analyzed area of a TaTO thin film.

The TOF-SIMS results for TaTO samples annealed in ^{18}O are shown in **Figure 4 (b)**. For both samples there is incorporation of oxygen. The decay of the $^{18}O/^{16}O$ ratio as a function of depth is well described by an exponential function in both cases (see the fitting lines in Figure 4 (b)). Note that while entering into the film, ^{18}O can also shift ^{16}O ions further into the sample, meaning that the ^{18}O profile does not fully correspond to the oxidation depth. Nonetheless, it is evident that UFA treatments performed under a higher concentration of ^{18}O (1000 vs. 80 ppm) resulted in (i) deeper ^{18}O penetration and (ii) larger ^{18}O concentration in proximity of the free surface of the TaTO film.

Although it is not possible to precisely determine the ^{18}O penetration depth one can still estimate that it should be limited to the first tens of nanometers of the thin films (Figure 4 (b)).

Consistently with the ^{18}O SIMS profiles, this assumption was confirmed by sputtering removal of the topmost surface layers (tens of nm) from the UFA TaTO film crystallized in

1000 ppm (orange curve in Figure 1). Interestingly, the removal of the top 30 nm of the film resulted in the recovery of ohmic contact characteristics and led to an almost totally recovered resistivity value, which was characterized by the same charge carrier concentration with respect to TaTO film UFA in 20 ppm, ($\rho = 8.76 \times 10^{-4} \Omega\text{cm}$, $n = 8.53 \times 10^{20} \text{cm}^{-3}$). Note also that as the Ta concentration is so large (5 at.%) any possible increase of the oxygen vacancy concentration owing to the sputtering process should be negligible for the change of resistivity.

4. Discussion

A standard annealing treatment performed at ambient pressure in N_2 (grade 99.999%, oxygen concentration nominally < 3 ppm) results in insulating TiO_2 -based thin films. This is the reason why in order to obtain highly conductive thin films a reducing atmosphere during a standard heat treatment is required. However, as shown above we found that during annealing a rather high content of oxygen can be tolerated as long as the heat treatment is extremely fast. Indeed, in terms of electrical properties, no significant differences (Table 1) were found upon ultra-fast-annealing treatments performed under reducing conditions (Ar/ H_2 mixture, measured oxygen concentration $< 10^{-20}$ ppm) or under rather oxidizing conditions (20 ppm O_2 in N_2) on TaTO (see Table 1).

Moreover, also the obtained structural (Figure 3 (a)), and optical properties (Figure 3 (b)) of all TiO_2 -based thin films demonstrate the possibility of achieving practically the same thin film quality of a standard vacuum annealing process (with an overall process time of about 180 minutes) with a 5 minutes UFA treatment under nitrogen at ambient pressure. This finding has obviously important consequences not only for technological applications but also for a better understanding of the charge carrier chemistry of anatase.

From *in-situ* resistance measurements during UFA treatments, *ex-situ* analyses (e.g. Hall effect measurements) as well as SIMS data collected upon annealing in an ^{18}O -containing

1 atmosphere, it is evident that the oxygen exchange (incorporation) is closely related to the
2 conductivity degradation of the TiO₂-based thin films during annealing.
3

4 In general, the oxygen exchange depends on temperature, oxygen partial pressure, and process
5 time. Since here the annealing temperature was kept constant throughout all experiments, we
6 varied O₂ content and annealing duration to investigate the role of oxygen incorporation. As
7 summarized in Table 1, for the given O₂ concentration (20 ppm for the N₂ flux employed) and
8 the peak temperature (460 °C) of the UFA treatment, we have observed no degradation of the
9 electrical conductivity compared to (i) UFA treatments carried out under reducing conditions
10 and, more importantly, (ii) to the standard vacuum annealing process. In contrast, extended
11 UFA treatments (exposure to 460 °C for 10 min at 20 ppm O₂) led to the degradation of the
12 electrical conductivity of both TaTO and TiO₂ thin films ($R_{T=25^{\circ}\text{C}} = 11 \Omega$ and 4965 Ω for
13 TaTO and TiO₂ respectively) with respect to the conventional UFA cycle ($R_{T=25^{\circ}\text{C}} = 6 \Omega$ and
14 96 Ω for TaTO and TiO₂ respectively). It is important to emphasize that despite the rather low
15 temperature (460 °C) and the limited duration of the heat treatment (10 min at 460 °C), the
16 change of the electrical properties is considerable: a factor 2 increase of the resistance for
17 TaTO and a factor 50 for TiO₂ (Figure s1). This further highlights the importance of the
18 oxygen exchange between anatase thin films and the environment as far as the electrical
19 properties are concerned.
20

21 Furthermore, it is worth noting that the very similar charge carrier density (see Table 1)
22 obtained with a standard annealing cycle performed in vacuum and the UFA treatment at 20
23 ppm O₂ strongly indicates that upon PLD deposition the reducing conditions of the standard
24 anneal do not create further oxygen vacancies (or at least not in a sufficient concentration to
25 effectively change the concentration of mobile electrons), but rather that the oxygen-poor
26 environment is useful for preventing oxygen incorporation during annealing. This is
27 consistent with the possibility of tuning the charge carrier density of vacuum annealed TaTO
28
29
30
31
32
33
34
35
36
37
38
39
40
41
42
43
44
45
46
47
48
49
50
51
52
53
54
55
56
57
58
59
60
61
62
63
64
65

1 thin films by adjusting the oxygen partial pressure during the room temperature PLD process
2 as shown in our previous work (see Figure 6 in reference^[12]).
3

4 As illustrated by XRD and optical microscopy data, during annealing the films become
5 crystalline. In the light of the above considerations, we propose that under such conditions the
6 amorphous TiO₂-based thin films undergoing the UFA treatment rapidly crystallize in the
7 anatase phase without (or, in the case of oxygen concentrations > 20 ppm, with limited)
8 oxygen incorporation from the surroundings, thus preventing the material from reaching
9 equilibrium with the annealing atmosphere. This means in turn that the final thin film
10 stoichiometry is in first approximation determined solely by the room temperature PLD
11 deposition conditions. In this context, it is important to consider the presence of region-A in
12 Figure 1, 2 and 4 (a), (see Section 3.2), in which the resistance changes clearly depend on the
13 oxygen partial pressure of the annealing environment for both doped and undoped TiO₂. We
14 interpret the different variations of R with T in this region as an indication of oxygen
15 incorporation occurring in the very first stages of the crystallization process. Previous studies
16 performed on amorphous undoped and Nb-doped TiO₂ thin films already pointed out that the
17 crystallization process can start with a sluggish rate at temperatures around 300 °C.^[13, 27, 30-35]
18
19 At higher temperatures ($T \geq 400$ °C), the crystallization process is faster, resulting in the
20 abrupt drop of the resistance as indicated by the region-B in Figure 1 and Figure 2. The order
21 of magnitude of the resistance drop in region-B for both TiO₂ and TaTO seems to be almost
22 independent of the oxygen partial pressure, i.e. mainly related to the mobility increase, while
23 going from amorphous TiO₂ to crystalline anatase (see Section 3.2). Consequently, this
24 suggests that the oxygen incorporation during annealing is mostly effective in the first stage
25 of the crystallization process (region-A), in which the crystallization rate of the process is still
26 rather sluggish.
27
28

29 Let us consider now the UFA treatments at 1000 ppm O₂ and in air. In both cases, we observe
30 that the detrimental effect on the electrical properties is notably different between doped and
31
32
33
34
35
36
37
38
39
40
41
42
43
44
45
46
47
48
49
50
51
52
53
54
55
56
57
58
59
60
61
62
63
64
65

undoped samples. This can be rationalized in terms of defect chemistry: while moving from a reducing environment (PLD thin films deposited at room temperature) into a rather oxidizing one (UFA treatment performed at a rather high oxygen concentration) the increase of resistivity is expected to be more pronounced for the undoped composition, since the annihilation of oxygen vacancies ($V_O^{\bullet\bullet}$ in the Kröger-Vink notation) and eventually titanium interstitials ($Ti_i^{\bullet\bullet\bullet\bullet}$) could severely reduce the electron concentration of the undoped material.^[36-39] In the case of Ta-doped TiO_2 instead, the high doping level (5 at.%) pins the electron concentration over a broad range of oxygen partial pressure ($n \sim 1.4 \times 10^{21} \text{ cm}^{-3}$ under the hypothesis of 100% Ta replacing Ti - Ta_{Ti}^{\bullet}) making the exposure to rather oxidizing conditions less problematic in terms of conductivity if an association/interplay among different defects is not taken in consideration. Nonetheless, in the donor-doped case, the concentration of negatively charged defects such as titanium vacancies ($V_{Ti}^{\prime\prime\prime}$) and oxygen interstitials ($O_i^{\prime\prime}$) is expected to be larger than in the undoped situation so that they might also contribute to decreasing the concentration of mobile electrons.^[24, 25, 36, 37, 40]

SIMS data acquired upon ^{18}O incorporation experiments prove that the oxygen insertion occurring during UFA at moderate O_2 concentration (80 ppm or 1000 ppm) is essentially limited to approximately the first tens of nm of the TaTO thin films (see Figure 4 (b)). This is nicely and independently confirmed by the removal of the surface of the thin films by sputtering: as the top 30 nm of the TaTO film were removed, the electrical conductivity was recovered and it was possible to verify that the charge carrier density matched the thin films subjected to UFA under 20 ppm O_2 . We have thus experimentally demonstrated the presence of a thin surface layer on top of the highly conducting film, which is characterized by a higher oxygen concentration and resistivity. This eventually leads to a non-ohmic contact behavior in the case of TaTO thin films, which were UFA-crystallized at 1000 ppm and 21% oxygen concentration. It is noteworthy that the equivalent samples crystallized under the same UFA conditions with the evaporated Ti/Au electrodes on top exhibit an ohmic behavior between the

1 electrode pads. This fact is consistent with oxygen penetration (and associated conductivity
2 reduction) limited to the topmost uncovered surface of the thin film, while oxygen cannot
3 reach the surface of the thin film underneath the Ti/Au evaporated contacts which therefore
4 remains highly conducting.
5
6

7
8
9 The collected evidence is in line with the above discussed TaTO defect chemistry: the
10 exposure of the material to rather oxidizing annealing conditions should (i) fill the existing
11 oxygen vacancies (which are supposed to be present in the pristine thin films because of the
12 reducing conditions employed during the room temperature PLD deposition) and (ii) possibly
13 enhance the concentration of other defects such as titanium vacancies and oxygen interstitials,
14 which can also act as ‘electron killers’.^[41] It is consequently reasonable to assume a
15 significant electron density reduction in the thin surface layer induced by the environmental
16 oxygen which is incorporated during the crystallization process, while the thin film beneath it
17 preserves its high conductivity (and its stoichiometry). From the technological point of view,
18 the presence of a thin layer characterized by a lower charge carrier concentration on top of the
19 TCO layer is usually the basic condition required in a solid state dye sensitized/perovskite-
20 based solar cell, in which the presence of a low charge carrier density selective layer is needed
21 on top of the TCO in order to avoid high recombination rates between the photogenerated
22 charge carriers.
23
24

25
26
27 Note that although the incorporation of nitrogen ions during the investigated UFA treatments
28 is very unlikely (for this reason nitriding processes are performed in NH₃ or N-containing
29 plasma rather than in N₂), nitrogen entering into anatase could substitute oxygen and act as an
30 acceptor (N'_O). This would further reduce the concentration of electrons, in addition to the
31 effect of the oxygen partial pressure which has been shown to be the ruling mechanism.^[42]
32
33

34
35
36 Finally, it is noteworthy how fast the crystallization process proceeds leading to the formation
37 of anatase grains with a typical lateral size of several micrometers within only few minutes.
38
39 This is due to the characteristic ‘explosive’ crystallization of TiO₂.^[12, 34, 35] This phenomenon
40
41
42
43
44
45
46
47
48
49
50
51
52
53
54
55
56
57
58
59
60
61
62
63
64
65

1 has been attributed to the latent heat released during TiO₂ crystallization, which is large
2 enough to result in a runaway process that continues until the amorphous material is
3 completely consumed.^[34] In our study, the lateral size distribution of the grains for both TiO₂
4 and TaTO thin films was found to be on the order of 10 μm for both the standard annealing
5 and the UFA treatments (actually, for the standard treatment a larger average size is observed
6 as shown by the optical microscopy images with polarized light reported in **Figure s3** in the
7 Supporting Information).

18 **5. Conclusion and Perspectives**

19 We have demonstrated how ultra-fast annealing (UFA) treatments can be used to crystallize
20 TiO₂-based thin films in the presence of mildly oxidizing conditions with an overall process
21 time of just 5 minutes.

22 In particular, our experimental findings show that UFA treatments performed at ambient
23 pressure in N₂ atmosphere (measured oxygen concentration of 20 ppm) allow for obtaining
24 TiO₂-based TCOs with excellent electrical conductivity and transparency. Actually, the
25 resulting properties are almost identical to those obtained through standard annealing
26 treatments performed under a reducing atmosphere (e.g. vacuum). This is due to the
27 possibility of avoiding and/or limiting (in a controlled way) oxygen incorporation during
28 ultra-fast annealing.

29 Finally, this process is potentially highly appealing for the fabrication of new generation
30 photovoltaic solar cells, in which TiO₂ already plays a key role (i.e. photoanode / selective
31 layer). By engineering the UFA crystallization process as a function of the oxygen
32 concentration in the annealing atmosphere and by finely controlling the oxygen penetration
33 depth, it is possible to obtain TaTO films with tunable electrical properties as a function of the
34 film depth. This reveals the possibility of fabricating an all-TaTO electrode, i.e. a TaTO TCO
35 film with a top selective layer created by the UFA process, in which it is possible to tune the

1 thickness of the selective layer as a function of the chosen device architecture in a single
2 deposition followed by the annealing process.^[18] This capability could reduce the number of
3 sharp interfaces among different materials (e.g. FTO – TiO₂) in several solar cell
4 configurations and consequently the possible presence of recombination centers^[43] or energy
5 barriers^[11] for a more efficient electron collection.
6
7
8
9
10

11 **Supporting Information**

12 Supporting Information is available from the Wiley Online Library or from the author.
13
14
15
16

17 **Acknowledgements**

18 The authors wish to thank Rotraut Merkle for preparing the ¹⁸O/¹⁶O mixtures and for helpful
19 discussions, Udo Klock for the fundamental contribution in the realization of the ultra-fast
20 annealing furnace, Andrea Ballabio for the current-voltage sweep measurements, Gennady
21 Logvenov and Georg Christiani for the useful discussion on resistivity measurement of multi-
22 layer structured thin films, and David Dellasega for the helpful discussion on the surface
23 sputtering experiments.
24
25
26

27 Received: ((will be filled in by the editorial staff))

28 Revised: ((will be filled in by the editorial staff))

29 Published online: ((will be filled in by the editorial staff))
30
31
32
33

- 34 [1] Z. Weng, H. Guo, X. Liu, S. Wu, K. W. K. Yeung, P. K. Chu, *RSC Adv.* **2013**, *3*,
35 24758.
36
37
38 [2] B. O'Regan, M. Grätzel, *Nature* **1991**, *353*, 737.
39
40
41 [3] M. M. Lee, J. Teuscher, T. Miyasaka, T. N. Murakami, H. J. Snaith, *Science* **2012**,
42 338, 643.
43
44
45 [4] I. Concina, A. Vomiero, *Small* **2015**, *11*, 1744.
46
47
48 [5] H. Tang, H. Berger, P. E. Schmid, F. Lévy, G. Burri, *Solid State Commun.* **1993**, *87*,
49 847.
50
51
52 [6] H. Tang, F. Lévy, H. Berger, P. E. Schmid, *Phys. Rev. B* **1995**, *52*, 7771.
53
54
55 [7] A. Hagfeldt, G. Boschloo, L. Sun, L. Kloo, H. Pettersson, *Chem. Rev.* **2010**, *110*,
56 6595.
57
58
59
60
61
62
63
64
65

- 1
2
3
4
5
6
7
8
9
10
11
12
13
14
15
16
17
18
19
20
21
22
23
24
25
26
27
28
29
30
31
32
33
34
35
36
37
38
39
40
41
42
43
44
45
46
47
48
49
50
51
52
53
54
55
56
57
58
59
60
61
62
63
64
65
- [8] T. Kirchartz, J. Bisquert, I. Mora-Severo, G. Garcia-Belmonte, *Phys. Chem. Chem. Phys.* **2015**, *17*, 4007.
- [9] N.-G. Park, *J. Phys. Chem. Lett.* **2013**, *4*, 2423.
- [10] Y. Furubayashi, T. Hitosugi, Y. Yamamoto, K. Inaba, G. Kinoda, Y. Hirose, T. Shimada, T. Hasegawa, *Appl. Phys. Lett.* **2005**, *86*, 252101.
- [11] H.J. Snaith, and M. Grätzel, *Adv. Mater.* **2006**, *18*, 1910.
- [12] P. Mazzolini, P. Gondoni, V. Russo, D. Chrastina, C. S. Casari, A. Li Bassi, *J. Phys. Chem. C* **2015**, *119*, 6988.
- [13] T. Hitosugi, A. Ueda, S. Nakao, N. Yamada, Y. Furubayashi, Y. Hirose, T. Shimada, T. Hasegawa, *Appl. Phys. Lett.* **2007**, *90*, 212106.
- [14] H. A. Huy, B. Aradi, T. Frauenheim, P. Deak, *J. Appl. Phys.* **2012**, *112*, 016103.
- [15] S. Lee, J. H. Noh, H. S. Han, D. K. Yim, D. H. Kim, J.-K. Lee, J. Y. Kim, H. S. Jung, K. S. Hong, *J. Phys. Chem. C* **2009**, *113*, 6878.
- [16] R. Ghosh, Y. Hara, L. Aibabaei, K. Hanson, S. Rangan, R. Bartynski, T. J. Meyer, R. Lopez, *ACS Appl. Mater. Interfaces* **2012**, *4*, 4566.
- [17] X. Lü, X. Mou, J. Wu, D. Zhang, L. Zhang, F. Huang, F. Xu, S. Huang, *Adv. Funct. Mater.* **2010**, *20*, 509.
- [18] D. Liu, T. L. Kelly, *Nat. Photon* **2014**, *8*, 133.
- [19] N. Yamada, T. Hitosugi, N. L. H. Hoang, Y. Furubayashi, Y. Hirose, S. Konuma, T. Shimada, T. Hasegawa, *Thin Solid Films* **2008**, *516*, 5754.
- [20] P. Deák, B. Aradi, T. Frauenheim, *Phys. Rev. B* **2011**, *83*, 155207.
- [21] A. Rusydi, S. Dhar, A. R. Barman, Ariando, D.-C. Qi, M. Motapothula, J. B. Yi, I. Santoso, Y. P. Feng, K. Yang, Y. Dai, N. L. Yakovlev, J. Ding, A. T. S. Wee, G. Neuber, M. B. H. Breese, M. Ruebhausen, H. Hilgenkamp, T. Venkatesan, *Philos. Trans. R. Soc. A* **2012**, *370*, 4927.
- [22] T. Yamamoto, T. Ohno, *Phys. Rev. B* **2012**, *85*, 033104.

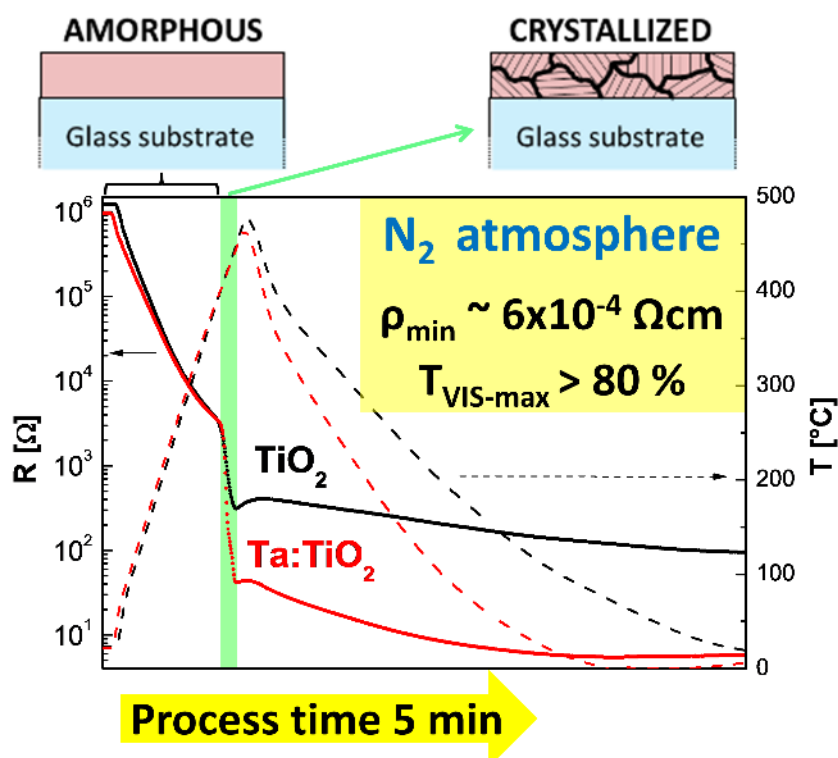
- 1
2
3
4
5
6
7
8
9
10
11
12
13
14
15
16
17
18
19
20
21
22
23
24
25
26
27
28
29
30
31
32
33
34
35
36
37
38
39
40
41
42
43
44
45
46
47
48
49
50
51
52
53
54
55
56
57
58
59
60
61
62
63
64
65
- [23] K.-C. Ok, Y. Park, K.-B. Chung, J.-S. Park, *Appl. Phys. Lett.* **2013**, *103*, 213501.
- [24] H.-Y. Lee, J. Robertson, *J. Appl. Phys.* **2013**, *113*, 213706.
- [25] S. Wang, L. Pan, J.-J. Song, W. Mi, J.-J. Zou, L. Wang, X. Zhang, *J. Am. Chem. Soc.* **2015**, *137*, 2975.
- [26] M. Setvin, C. Franchini, X. Hao, M. Schmid, A. Janotti, M. Kaltak, C. G. Van de Walle, G. Kresse, U. Diebold, *Phys. Rev. Lett.* **2014**, *113*, 086402.
- [27] T. Leichtweiss, R. A. Henning, J. Koettgen, R. M. Schmidt, B. Hollander, M. Martin, M. Wuttig, J. Janek, *J. Mater. Chem. A* **2014**, *2*, 6631.
- [28] S. Okazaki, J. Ohkubo, S. Nakao, Y. Hirose, T. Hitosugi, T. Hasegawa, *Jpn. J. Appl. Phys.* **2012**, *51*, 118003.
- [29] K. Ellmer, *Nat Photon* **2012**, *6*, 809.
- [30] N. L. H. Hoang, N. Yamada, T. Hitosugi, J. Kasai, S. Nakao, T. Shimada, T. Hasegawa, *Appl. Phys. Express* **2008**, *1*, 1150011.
- [31] J. H. Park, H. K. Kim, H. Lee, S. Yoon, C. D. Kim, *Electrochem. Solid State Lett.* **2010**, *13*, J53.
- [32] N. L. H. Hoang, Y. Hirose, S. Nakao, T. Hasegawa, *Appl. Phys. Express* **2011**, *4*, 105601.
- [33] J.-H. Park, S. J. Kang, S.-I. Na, H. H. Lee, S.-W. Kim, H. Hosono, H.-K. Kim, *Sol. Energ. Mat. Sol. Cells* **2011**, *95*, 2178.
- [34] V. Pore, M. Ritala, M. Leskelä, T. Saukkonen, M. Järn, *Cryst. Growth Des.* **2009**, *9*, 2974.
- [35] C. Yang, Y. Hirose, S. Nakao, N. L. H. Hoang, T. Hasegawa, *Appl. Phys. Lett.* **2012**, *101*, 052101.
- [36] P. Knauth, H. L. Tuller, *J. Appl. Phys.* **1999**, *85*, 897.
- [37] A. Weibel, R. Bouchet, P. Knauth, *Solid State Ion.* **2006**, *177*, 229.
- [38] P. Deák, B. Aradi, T. Frauenheim, *Phys. Rev. B* **2012**, *86*, 195206.

- 1 [39] J. Engel, S. R. Bishop, L. Vayssieres, H. L. Tuller, *Adv. Funct. Mater.* **2014**, *24*, 4952.
2
3 [40] S. Zhang, S. B. Ogale, W. Yu, X. Gao, T. Liu, S. Ghosh, G. P. Das, A. T. S. Wee, R.
4 L. Greene, T. Venkatesan, *Adv. Mater.* **2009**, *21*, 2282.
5
6 [41] J. Robertson, S. J. Clark, *Phys. Rev. B* **2011**, *83*, 075205.
7
8 [42] J. Shi, D.-K. Lee, H.-I. Yoo, J. Janek, K.-D. Becker, *Phys. Chem. Chem. Phys.* **2012**,
9 *14*, 12930.
10
11 [43] E. J. Juarez-Perez, M. Wußler, F. Fabregat-Santiago, K. Lakus-Wollny, E. Mankel, T.
12 Mayer, W. Jaegermann, I. Mora-Sero, *J. Phys. Chem. Lett.* **2014**, *5*, 680.
13
14
15
16
17
18
19
20
21
22
23
24
25
26
27
28
29
30
31
32
33
34
35
36
37
38
39
40
41
42
43
44
45
46
47
48
49
50
51
52
53
54
55
56
57
58
59
60
61
62
63
64
65

We report on an ultra-fast crystallization process of transparent and conducting TiO_2 and Ta-doped TiO_2 thin films in nitrogen atmosphere at ambient pressure. *In-situ* resistance measurements in controlled annealing atmospheres demonstrate the possibility to finely control their electrical properties in an extremely fast process highly appealing for new generation solar cell devices.

P. Mazzolini, T. Acartürk, D. Chrastina, U. Starke, C.S. Casari, G. Gregori and A. Li Bassi**

Controlling the Electrical Properties of Undoped and Ta-doped TiO_2 Polycrystalline Films via Ultra-Fast Annealing Treatments

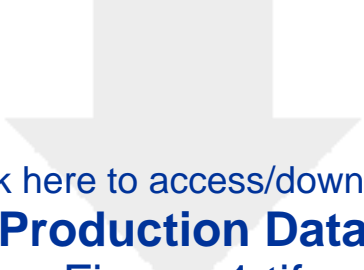




Click here to access/download

Supporting Information

MazzoliniP_AdvanceElectronicMaterials_SupportingInfo.
docx



Click here to access/download

Production Data

Figure_1.tif

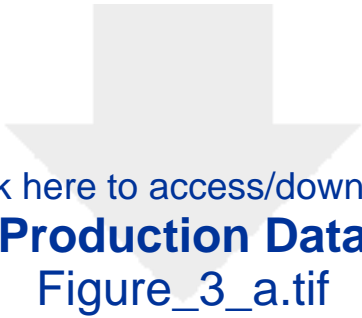




[Click here to access/download](#)

Production Data

Figure_2.tif

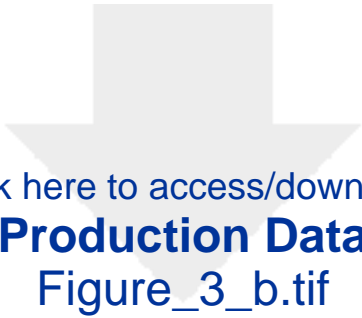


Click here to access/download

Production Data

Figure_3_a.tif






Click here to access/download

Production Data

Figure_3_b.tif






Click here to access/download

Production Data

Figure_4_a.tif





Click here to access/download

Production Data

Figure_4_b.tif





Click here to access/download
Production Data
TOC.tif